Materials Science and Engineering B107 (2004) 198–203

www.elsevier.com/locate/mseb

Kinetics of {3 1 1} defect dissolution in silicon-on-insulator (SOI)

A.F. Saavedra [a,*], K.S. Jones [a], M.E. Law [b], K.K. Chan [c]

[a] *Department of Materials Science and Engineering, SWAMP Center, University of Florida, Gainesville, FL 32611, USA*
[b] *Department of Electrical and Computer Engineering, SWAMP Center, University of Florida, Gainesville, FL 32611, USA*
[c] *Research Division, IBM Semiconductor Research and Development Center, Yorktown Heights, NY 10598, USA*

Received 29 August 2003

Abstract

The reaction kinetics of {3 1 1} defect dissolution in SIMOX, SOITEC and bulk silicon materials have been investigated. The effects of implant energy and surface silicon thickness on the activation energy for {3 1 1} dissolution have been measured using quantitative TEM (QTEM). SOI wafers having surface silicon thickness of 750 and 1450 Å were implanted with Si^+ ions at 15–48.5 keV, 1×10^{14} cm^{-2}. Furnace and RTA anneals were performed at temperatures ranging from 700 to 825 °C. Quantitative TEM was used to monitor the trapped interstitial dose in {3 1 1} defects. The activation energy for {3 1 1} dissolution was found to decrease as the surface silicon thickness decreased, suggesting a lower activation barrier as the implant damage approaches the surface silicon/buried oxide (BOX) interface. However, the 1450 Å SOI had similar dissolution kinetics to the bulk silicon for all of the implants studied suggesting the reduced activation barrier is likely due to recombination at the surface Si/BOX interface.

Keywords: Transmission electron microscopy; Silicon; Silicon-on-insulator; Solid-solid interfaces; Doping and impurity implantation; Defect formation

1. Introduction

By now, the advantages of silicon-on-insulator (SOI) as a substrate material for complementary metal-oxide semiconductor (CMOS) fabrication have been well documented [1]. However, the present understanding of the role of point defects generated by ion implantation on dopant diffusion in SOI is fairly limited. In order to model and develop advanced SOI devices, these interactions need to be better understood.

At present, {3 1 1} defects are believed to be the major source of transient enhanced diffusion (TED) of dopants in bulk silicon [2]. These defects are able to maintain a supersaturation of interstitials until they are dissolved at sufficiently high annealing temperatures. This effect can often lead to unacceptable junction depths in bulk silicon devices. Modeling of {3 1 1} defect [3–6] and dislocation loop [7] behavior has greatly improved the validity of process simulators. Unfortunately, up to this point no such models exist for SOI.

Although junction formation in SOI is fairly straightforward, point defects are likely to still play a role in dopant segregation around the surface silicon/buried oxide (BOX) interface [8,9]. This phenomenon is likely to be critical as SOI devices are scaled. Previous studies have shown that dislocation loop [10] and {3 1 1} [11] nucleation can depend strongly on the SOI thickness and/or implant energy. The present study set out to investigate the reaction kinetics of {3 1 1} defect dissolution in SOI, and then compare it to bulk silicon.

2. Experimental

Separation by implantation of oxygen (SIMOX) and bonded (SOITEC) wafers were used, along with Czochralski wafers, in the experiment. All wafers were p-type, 200 mm, {0 0 1}, with a BOX thickness of 1300 Å. Some of the 1450 Å SOI wafers were thinned to 750 Å using oxidation and etching in dilute hydrofluoric acid (10:1). Ion implantation was done at angles of 7° tilt and 22° twist; implants consisted of $^{28}Si^+$ ions at a non-amorphizing dose of 10^{14} cm^{-2}. The implant energies were 15, 30, and 48.5 keV for the 1450 Å SOI and bulk silicon. For the 750 Å SOI,

* Corresponding author. Tel.: +1-352-392-1030; fax: +1-352-392-8381.
E-mail address: asaav@ufl.edu (A.F. Saavedra).

0921-5107/$ – see front matter © 2003 Published by Elsevier B.V.
doi:10.1016/j.mseb.2003.11.004

only the 15 and 30 keV energies were performed in order to prevent substantial dose loss to the BOX. Furnace anneals were performed at 700 and 750 °C in a Thermolyne quartz tube furnace with a nitrogen ambient. An AG Associates rapid thermal annealing (RTA) system was used in order to provide controllability for shorter anneals at 825 °C. The methodology for determining the anneal times is described in the following paragraph. Plan-view transmission electron microscopy (PTEM) SOI specimens were fabricated by mechanical grinding with 15 μm alumina, followed by etching using HNO_3:HF 3:1. Buffered oxide etching (6:1) was used to help remove the BOX from the SOI specimens. A JEOL 200CX TEM operating at accelerating voltage of 200 kV was used for imaging under weak beam dark field g(3g) conditions using a g_{220} diffracted beam. Micrographs were taken at 50,000× and then printed at a total magnification of 150,000× so that quantitative TEM (QTEM) could be performed. QTEM was used to measure the trapped interstitial dose, defect size, and defect density.

The trapped interstitial decay for {3 1 1} defects varies exponentially with time[2] according to Eq. (1),

$$\mathrm{Si_I} = \mathrm{Si_I}(0)\mathrm{e}^{-t/\tau} \quad (1)$$

where $\mathrm{Si_I}$ is the trapped interstitial dose, $\mathrm{Si_I}(0)$ the pre-exponential factor, t the time, and τ the decay time constant. This time constant can be shown to follow an Arrhenius expression [12], such as in Eq. (2),

$$\tau = \tau_0 \mathrm{e}^{-E_a/kT} \quad (2)$$

where τ_0 is the pre-exponential, E_a the activation energy for {3 1 1} dissolution, k Boltzmann's constant, and T the temperature. Anneal times were determined by assuming an activation energy of 3.7 eV [13] for {3 1 1} dissolution, corresponding closely with previous studies of enhanced diffusion and extended defect evolution [14]. Thus, if one determines the time for annealing at a particular temperature an equivalent time can be determined at another temperature by equating the ratio of the activation rates. This allows for observation of similar microstructures at different annealing temperatures, rather than a simple isochronal sequence. For example,

$$t_2 = \left[\frac{\tau_1}{\tau_2}\right] \times t_1 = \left[\frac{\mathrm{e}^{-3.7\,\mathrm{eV}/kT_1}}{\mathrm{e}^{-3.7\,\mathrm{eV}/kT_2}}\right] \times t_1 \quad (3)$$

where t_1 is the annealing time at temperature T_1 and t_2 is the unknown time for temperature T_2. Perhaps the most common temperature for observing {3 1 1} defect evolution is 750 °C, since the {3 1 1}s do not dissolve too fast or slow. Thus, 750 °C was used as a baseline for determining the equivalent annealing times at 700 and 825 °C. Table 1 shows equivalent annealing times for 700, 750 and 825 °C based on this procedure.

Table 1
Equivalent annealing times assuming 3.7 eV activation energy for {3 1 1} defects in bulk Si

Temperature (°C)	Time				
700	40 min	122 min	244 min	489 min	979 min
750	5 min	15 min	30 min	60 min	120 min
825	18 s	55 s	110 s	220 s	440 s

Table 2
Ion range statistics determined using UT-Marlowe and SRIM simulations

Energy (keV)	UT-Marlowe R_p (Å)	SRIM R_p (Å)
15	180	240
30	330	446
48.5	550	700

R_p: projected range.

Table 3
Dose loss for 750 and 1450 Å SOI determined using UT-Marlowe

Energy (keV)	750 Å SOI dose loss (%)	1450 Å SOI dose loss (%)
15	3	<1
30	10	1
48.5	30	3

3. Results

Table 2 shows the as-implanted stopping range statistics for the Si^+ implants obtained from UT-Marlowe [15] and SRIM [16]. Dose loss due to implant overlap with the buried oxide was calculated by truncating the implant profile obtained from UT-Marlowe at the surface Si/BOX interface and integrating only the ions left in the surface silicon layer (Table 3). This value was then subtracted from the actual implanted dose of $10^{14}\,\mathrm{cm}^{-2}$.

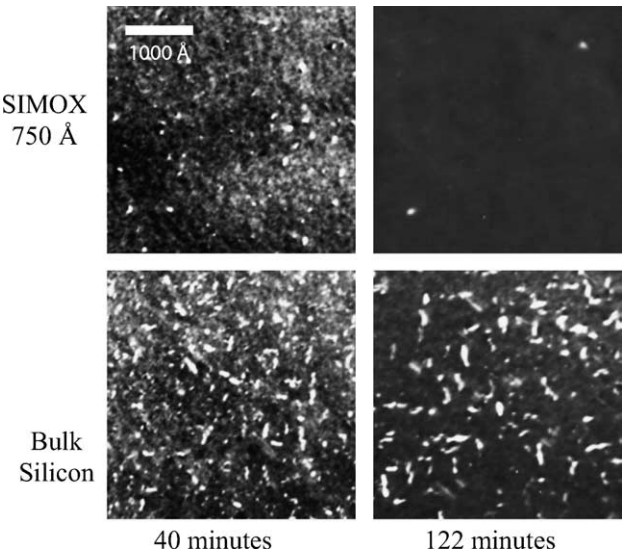

Fig. 1. Weak beam dark field micrographs of 750 Å SIMOX and bulk silicon for Si^+, 30 keV, $10^{14}\,\mathrm{cm}^{-2}$ implants after annealing at 700 °C for 40 and 122 min.

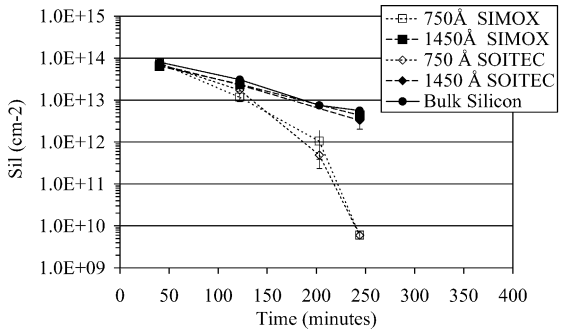

(a) 700 °C

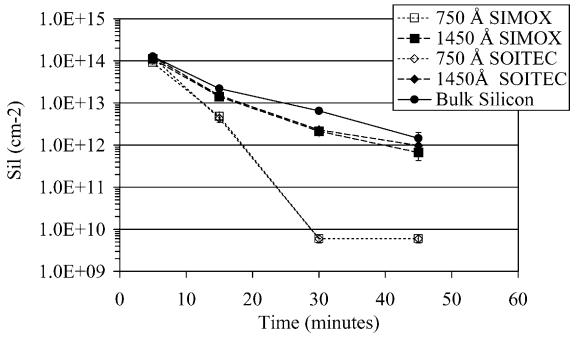

(b) 750 °C

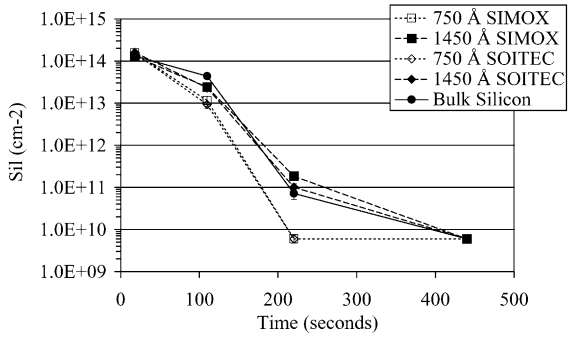

(c) 825 °C

Fig. 2. Concentration of trapped interstitials in {3 1 1} defects for Si^+, 15 keV, 10^{14} cm^{-2} annealed at (a) 700 °C, (b) 750 °C, and (c) 825 °C (*note*: $Si_I = 6 \times 10^9$ cm^{-2} is TEM detection limit).

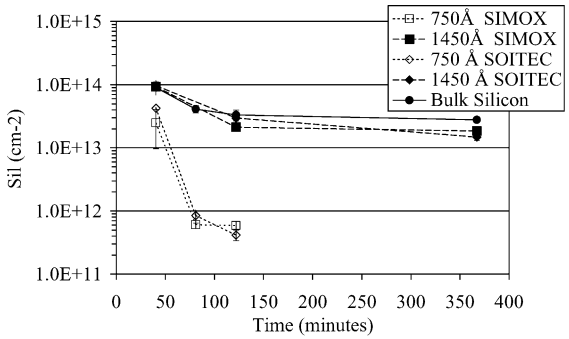

(a) 700 °C

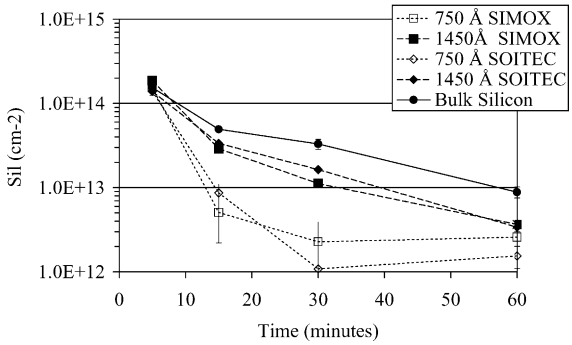

(b) 750 °C

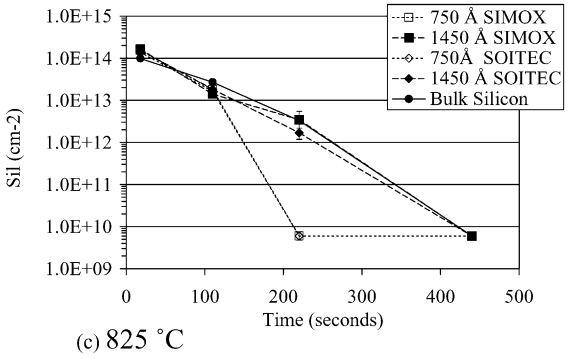

(c) 825 °C

Fig. 3. Concentration of trapped interstitials in {3 1 1} defects for Si^+, 30 keV, 10^{14} cm^{-2} annealed at: (a) 700 °C, (b) 750 °C, and (c) 825 °C.

Fig. 1 shows a series of micrographs comparing the defect evolution between 750 Å SIMOX and bulk silicon for the 30 keV implant energy. Upon annealing, this non-amorphizing implant evolves into type 1 extended defects consisting of {3 1 1} defects and extrinsic dislocation loops [17]. At early times, a high density of dot defects appear, which may or may not be small {3 1 1} defects. As annealing proceeds, the {3 1 1} defects grow and then either dissolve or unfault [18] to form dislocation loops. The {3 1 1} defects are clearly smaller in the 750 Å SIMOX samples than in the bulk Si.

Figs. 2–4 show the time dependency of the trapped interstitial dose in {3 1 1}s for the three implant energies at the three temperatures. In each of the cases, the {3 1 1} defects appear to be less stable in the 750 Å SOI compared to the 1450 Å SOI and bulk Si. As the implant energy is increased to 48.5 keV, the {3 1 1} defects in the 1450 Å SOI appear to be less stable than bulk Si. These phenomena have been discussed previously by Saavedra et al. [11]. It should be noted that all trapped interstitials are assumed to be in {3 1 1} defects at the first time point for each of the three temperatures. The validity of this assumption is discussed below.

{3 1 1} defects are metastable in the sense that they can undergo an unfaulting reaction to form a dislocation loop, but a dislocation loop cannot form a {3 1 1}. It is believed that {3 1 1} defects nucleate from sub-microscopic interstitial clusters (SMICs) [19]. Thus, it makes sense that the small dot

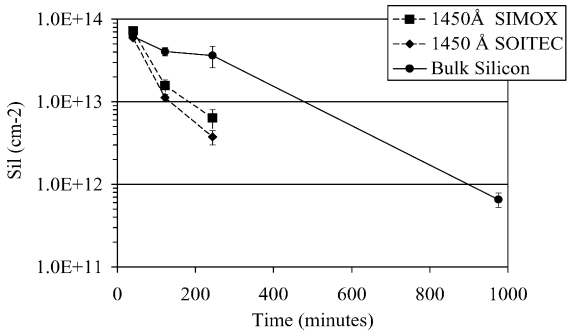

(a) 700 °C

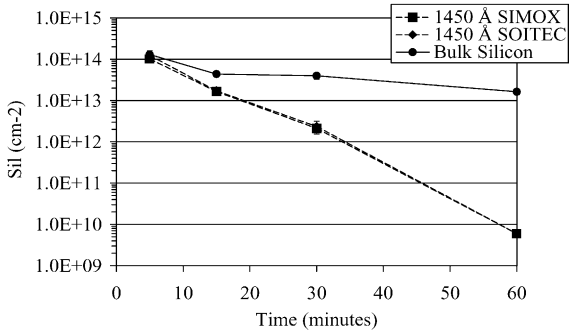

(b) 750 °C

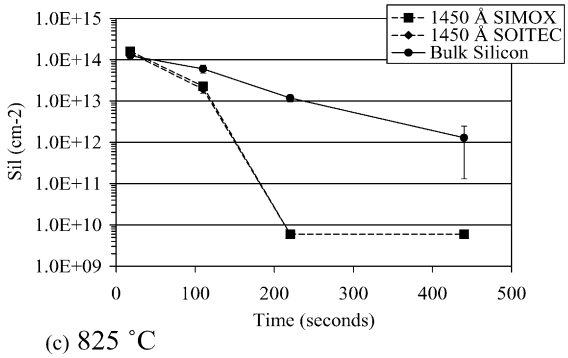

(c) 825 °C

Fig. 4. Concentration of trapped interstitials in {3 1 1} defects for Si^+, 48.5 keV, 10^{14} cm^{-2} annealed at: (a) 700 °C, (b) 750 °C, and (c) 825 °C.

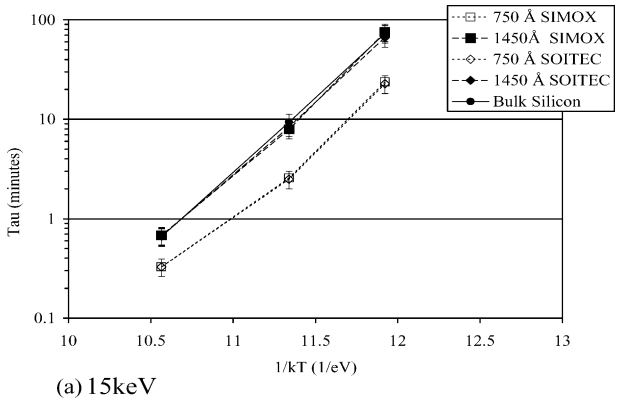

(a) 15keV

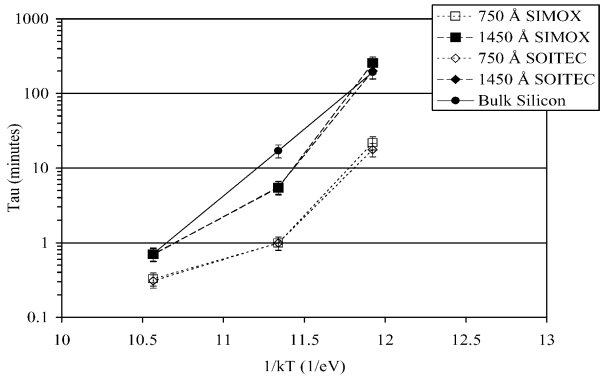

(b) 30 keV

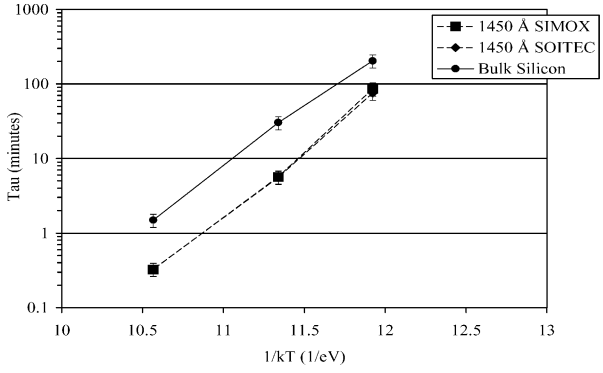

(c) 48.5 keV

Fig. 5. Plot of time constant as function of $1/kT$ for: (a) 15 keV, (b) 30 keV, and (c) 48.5 keV.

defects at early times are more similar to the {3 1 1} rather than a stable dislocation loop, since they preclude {3 1 1} formation. The dot defects do not appear to simply skip {3 1 1} formation and nucleate into stable dislocation loops.

Fig. 5 shows the plot of the time constant, τ, for {3 1 1} dissolution versus $1/kT$. Time constants were obtained by fitting the trapped interstitial decay curves in Figs. 2–4 with an exponential function of the form in Eq. (1). This was done using a least squares fit through the data points. Similarly, fitting the curves in Fig. 5 with an exponential yields the activation energy, E_a, according to Eq. (2). These values appear in Table 4. Standard deviation, σ, was calculated by fitting exponential functions through the maximum and minimum of the error bars in the first and last $1/kT$ value, respectively. The activation energy for {3 1 1} dissolution in the 750 Å SOI is slightly less than the 1450 Å SOI and bulk Si for the 15 and 30 keV implants. However, E_a for the 1450 Å SOI is similar to bulk Si at each of the implant energies. No difference in E_a due to the type of SOI substrate can be seen in the data.

4. Discussion

The data from Figs. 1–4 agree with previous studies of dislocation loop and {3 1 1} evolution in SOI [10,11]. As the implant energy increases, or the surface silicon thickness

Table 4
Extracted activation energies from Fig. 5 for SIMOX, SOITEC and bulk Si

Energy (keV)	Activation energy, E_a (eV)				
	SIMOX 750 Å	SIMOX 1450 Å	SOITEC 750 Å	SOITEC 1450 Å	Bulk Si
15	3.13 ± 0.3	3.45 ± 0.30	3.10 ± 0.30	3.38 ± 0.30	3.47 ± 0.3
30	3.03 ± 0.33	4.26 ± 0.30	2.9 ± 0.3	4.1 ± 0.3	4.13 ± 0.3
48.5		4.09 ± 0.30		3.99 ± 0.3	3.64 ± 0.3

decreases, it becomes easier for interstitials to recombine at the surface Si/BOX interface. It has been hypothesized that damage to the interface strongly affects the ability of interstitials to recombine [10]. Thus, as the implant energy increases more of the incident ions reach the BOX increasing the damage to the interface. Interstitials have a high diffusivity [20] at the temperatures under investigation, so it could be set forth that recombination at the interface is a reaction rate-limited process. In other words, interfacial recombination is limited by the ability of interstitials to dissociate from the {3 1 1} rather than their diffusion to the interface. This goes along with the observations of Li and Jones [18] and the model of Law and Jones [3].

The decrease in the activation energy in the 750 Å SOI indicates a reduced barrier for interstitial dissociation from the {3 1 1} defect. Whether or not this is the result of interstitial recombination or simply due to a reduction of defect size is unclear. It has been shown that smaller {3 1 1}s dissolve faster than larger {3 1 1}s [18]. However, a reduction in defect size should not change the activation energy for {3 1 1} dissolution. Another process, e.g. recombination, could change the activation energy.

The thermal behavior of {3 1 1}s in thick SOI is the same as bulk Si, as long as the implant energy is not sufficiently high. Smaller {3 1 1} defects are observed in the 1450 Å SOI at the 48.5 keV implant energy, yet the activation energy is approximately the same as bulk Si. This would also lend support to the interstitial recombination at the surface Si/BOX interface theory, since the smaller defects dissolve faster. However, the defect layer is far enough away from the interface that the activation energy for dissolution is not affected.

It can be theorized that the activation energy will continue to decrease if the surface Si thickness is scaled further. This may result in a nearly athermal behavior of the {3 1 1} defect in SOI as the defect layer approaches the surface Si/BOX interface. King et al. [21] found a activation energy of approximately 1.0 eV for defects in the proximity of the surface in bulk Si. A proximity investigation in SOI is difficult due to the large dose losses that occur if the project range of the implant is placed in the vicinity of the surface Si/BOX interface. This could potentially prevent extended defects from even forming in SOI, unless the dose is sufficiently high.

5. Conclusions

The reaction kinetics of {3 1 1} defect dissolution in SOI have been studied via quantitative TEM. A reduction in defect size leads to an enhanced decay rate of {3 1 1}s in SOI. Thinning of the surface silicon layer results in a decrease in the activation energy of {3 1 1} dissolution in SOI. Increasing the implant energy also results in a reduction in the activation energy in 750 Å SOI. It is hypothesized that interstitial recombination at the surface Si/BOX interface is responsible for the reduction in activation energy when the defect layer is within ∼500 Å. It is also proposed that the dissolution kinetics will tend towards athermal behavior as the implant damage is placed closer to the interface.

Acknowledgements

The efforts of the Advanced Si Technology Laboratory at the IBM T.J. Watson Research Center for material processing is appreciated. The Major Analytical Instrumentation Center in the UF Materials Science Department is acknowledged for the use of TEM. This work was funded by the Semiconductor Research Corporation (SRC) under task 819.001. The authors acknowledge IBM for directly funding the task.

References

[1] S. Cristoloveanu, S.S. Li, Electrical Characterization of Silicon-on-Insulator Materials and Devices, first ed., Kluwer Academic Publishers, Boston, 1995, pp. 1–4.
[2] D.J. Eaglesham, P.A. Stolk, H.-J. Gossmann, J.M. Poate, Appl. Phys. Lett. 65 (1994) 2305.
[3] M.E. Law, K.S. Jones, IEDM Technical Digests (2000) 511.
[4] G. Hobler, C.S. Rafferty, S. Senkader, SISPAD (1997) 73.
[5] A.H. Gencer, S.T. Dunham, J. Appl. Phys. 81 (1997) 631.
[6] C.S. Rafferty, G.H. Gilmer, M. Jaraiz, D. Eaglesham, H.-J. Gossmann, Appl. Phys. Lett. 68 (1996) 2395.
[7] I. Avci, M.E. Law, E. Kuryliw, K.S. Jones, IEDM Technical Digests (2001) 835.
[8] H. Park, E.C. Jones, P. Ronsheim, C. Cabral Jr., C. D'Emic, G.M. Cohen, R. Young, W. Rausch, IEDM Technical Digests (1999) 337.
[9] H.-H. Vuong, H.-J. Gossmann, L. Pelaz, G.K. Celler, D.C. Jacobson, D. Barr, J. Hergenrother, D. Monroe, V.C. Venezia, C.S. Rafferty, S.J. Hillenius, J. McKinley, F.A. Stevie, C. Granger, Appl. Phys. Lett. 75 (1999) 1083.
[10] A.F. Saavedra, J. Frazer, K.S. Jones, I. Avci, S.K. Earles, M.E. Law, E.C. Jones, J. Vac. Sci. Technol. B 20 (2002) 2243.
[11] A.F. Saavedra, K.S. Jones, M.E. Law, K.K. Chan, J. Electrochem. Soc., in press.
[12] S.C. Jain, W. Schoenmaker, R. Lindsay, P.A. Stolk, S. Decoutere, M. Willander, H.E. Maes, J. Appl. Phys. 91 (2002) 8919.
[13] S. Solmi, F. Baruffaldi, R. Canteri, J. Appl. Phys. 69 (1991) 2135.

[14] J. Li, P. Keys, J. Chen, M.E. Law, K.S. Jones, C. Jasper, Mater. Res. Soc. Symp. Proc. 568 (1999) 175.
[15] UT-Marlowe Version 5.0, University of Texas, Austin.
[16] J.F. Ziegler, SRIM, 2000.
[17] K.S. Jones, S. Prussin, E.R. Weber, Appl. Phys. A 45 (1988) 1.
[18] J. Li, K.S. Jones, Appl. Phys. Lett. 73 (1998) 3748.
[19] S. Coffa, S. Libertino, C. Spinella, Appl. Phys. Lett. 76 (2000) 321.
[20] S.M. Hu, Mater. Sci. Eng. R 13 (1994) 105.
[21] A.C. King, A.F. Gutierrez, A.F. Saavedra, K.S. Jones, J. Appl. Phys. 93 (2003) 203.